PREPARATION AND TUNABLE LUMINESCENCE PROPERTIES OF Tb^{3+}-DOPED ZINC-ALUMINUM HYDROTALCITE-LIKE COMPOUNDS**

L. H. Zhang*, Y. L. Li, Y. B. Zhou, C. Y. Zhang

School of Chemistry and Environmental Engineering at Pingdingshan University, Pingdingshan, China; e-mail: 15290759930@139.com

Tb^{3+}-doped Zn-Al (ZnAlTb) hydrotalcites with tunable blue-green emission synthesized by co-precipitation. The compositions and properties of the samples were characterized by X-ray diffraction (XRD), Fourier-transform infrared spectroscopy (FTIR), and photoluminescence. XRD and FTIR results indicate that the samples were in a pure hydrotalcite-like phase. The fluorescence spectra indicate that the ZnAl hydrotalcite exhibited blue fluorescence at 350–450 nm. Under an excitation wavelength of 231 nm, ZnAlTb hydrotalcite exhibited the characteristic green emission of $^5D_0$–^7F_J of Tb^{3+}, and the fluorescence lifetime of the sample was 0.8442 ms. At different excitation wavelengths, ZnAlTb hydrotalcites can exhibit emission from green to blue wavelengths, which indicates that ZnAlTb hydrotalcites are potential multicolor functional materials.

Keywords: *Zn-Al hydrotalcites, Tb^{3+}-doped Zn-Al hydrotalcites, luminescence properties, multicolor.*

ПОЛУЧЕНИЕ И ЛЮМИНЕСЦЕНТНЫЕ СВОЙСТВА ПОДОБНЫХ Zn-Al-ГИДРОТАЛЬЦИТУ СОЕДИНЕНИЙ, ЛЕГИРОВАННЫХ ИОНАМИ Tb^{3+}

L. H. Zhang*, Y. L. Li, Y. B. Zhou, C. Y. Zhang

УДК 535.37

Университет Пиндиншань, Пиндиншань, Китай; e-mail: 15290759930@139.com

(Поступила 12 августа 2021)

Легированные ионами Tb^{3+} гидротальциты Zn-Al (ZnAlTb) с перестраиваемым сине-зеленым излучением синтезированы путем совместного осаждения. Состав и свойства образцов охарактеризованы с помощью рентгеновской дифракции, ИК-Фурье-спектроскопии и фотолюминесценции. Результаты рентгенографии и ИК-Фурье-спектроскопии свидетельствуют о том, что образцы находятся в чистой гидротальцитоподобной фазе. Показано, что гидротальцит ZnAl проявляет синюю флуоресценцию при 350—450 нм. При возбуждении с λ = 231 нм для гидротальцита ZnAlTb наблюдается характерное зеленое излучение Tb^{3+} на переходе $^5D_0$–^7F_J с временем жизни флуоресценции 0.8442 мс. При различных длинах волн возбуждения гидротальциты ZnAlTb могут проявлять излучение от зеленых до синих длин волн. Подтверждено, что гидротальциты ZnAlTb являются потенциальными многоцветными функциональными материалами.

Ключевые слова: *гидротальциты Zn-Al, легированные ионами Tb^{3+} гидротальциты Zn-Al, люминесцентные свойства, многоцветность.*

Introduction. The unique 4*f* electronic structure of rare-earth elements contributes to their luminescence. Such elements can emit light from the near-ultraviolet (UV) to far-infrared. Therefore, materials based on rare-earth elements are a rich source of luminescent materials [1–3]. The emission of Tb^{3+} is mainly from the $^5D_4 \rightarrow {}^7F_J$ (J = 0–6) transition. Therefore, Tb^{3+}-doped phosphors are an active area of research. For example, Sun et al. used a high-temperature solid-state method to prepare a $CaLuBO_4$:Tb^{3+} yellow–

**Full text is published in JAS V. 89, No. 4 (http://springer.com/journal/10812) and in electronic version of ZhPS V. 89, No. 4 (http://www.elibrary.ru/title_about.asp?id=7318; sales@elibrary.ru).

green phosphor that is suitable for UV excitation [4]. Seiya et al. synthesized green-emitting Tb^{3+}-doped pollucite $(Cs_{1-3x}Tb_x)AlSi_2O_6$ (x = 0.01–0.13) phosphors with emission at ~543 nm under excitation at 238 nm [5]. Zhao et al. reported a blue-emitting $Sr_5(PO_4)_2SiO_4:Ce^{3+},Tb^{3+}$ phosphor; the samples exhibited a wide and strong emission band located at 405 nm [6]. Mi et al. synthesized a series of $SrMg_2(PO_4)_2:Ce^{3+},Tb^{3+}$ phosphors with tunable emission spectra of blue–green light by controlling the dopant concentration [7]. Vijay et al. reported a Tb^{3+}-activated $Sr_2P_2O_7$ green phosphor under vacuum-UV and UV excitation for plasma display panel applications [8]. Layered double hydroxides (LDHs) are commonly termed Mg–Al hydrotalcites. Metal cations with a suitable ionic radius (close to the 0.072-nm ionic radius of Mg^{2+}) and charge number can form hydrotalcite-like compounds (HTlcs). The general formula of HTlcs is $[M^{II}_{1-x}M^{III}_x(OH)_2]^{x+}(A^{n-})_{x/n}$ mH_2O. Here, M^{II} is a divalent metal cation such as Mg^{2+}, Zn^{2+}, Ni^{2+}, or Cu^{2+}; M^{III} is a trivalent metal cation such as Al^{3+}, Cr^{3+}, Fe^{3+}, or Sc^{3+}; A^{n-} is an inorganic or organic ion such as CO_3^{2-}, NO_3^-, PO_4^{3-}, Cl^-, SO_4^{2-}, $C_6H_4(COO^-)_2$, or a complex anion. When x is between 0.17 and 0.33, LDHs with a complete structure can be generated [9–11]. Co-precipitation is a common method for preparing HTlcs because of its simple operation, the ease with which one can control the precipitation, and low energy input. In recent years, fluorescent materials based on hydrotalcite or hydrotalcite-like materials have become an active area of research. For example, Song et al. prepared fluorescent films of a $Na_9[EuW_{10}O_{36}]/Mg_2Al$–LDH nanocomposite by layer-by-layer assembly [12]. Chen et al. reported Mg-Al-Eu ternary hydrotalcite-like LDHs with a $^5D_0$–^7F_J transition (J = 1–4) of Eu^{3+} ions, with the strongest emission for J = 2 [13]. Chen et al. synthesized Mg-Al-Tb ternary hydrotalcite-like LDHs by co-precipitation [14]. In the [15–18] a Zn-Al layered double hydroxide was prepared. Herein, Tb^{3+}-doped Zn-Al HTlcs were prepared by coprecipitation. The photoluminescence properties of ZnAl hydrotalcite and Tb^{3+}-doped ZnAl hydrotalcite were studied.

Experimental. Analytical grade zinc sulfate ($ZnSO_4 \cdot 7H_2O$) and aluminum sulfate [$Al_2(SO_4)_2 \cdot 18H_2O$] were obtained from Beijing Chemical Reagent Factory (Beijing, China). $Tb_2(SO_4)_3$ (99.99% pure) was obtained from Shangdong Desheng (Shandong, China). ZnAl HTlcs were synthesized by co-precipitation. Zinc sulfate and aluminum sulfate were used as raw materials to prepare mixed salt solutions with different mole ratios of Zn^{2+}/Al^{3+}. The pH was adjusted to 8–9 with aqueous sodium hydroxide. Then, the precipitation was aged at 65°C for 24 h. The samples were centrifuged and dried at 60°C for 24 h. The synthesis of Tb^{3+}-doped ZnAl HTlcs was the same as described, but an appropriate quantity of $Tb_2(SO_4)_2$ was added to replace some of the Al^{3+}. Phase identification was performed by X-ray diffraction (XRD; Bruker, Japan). The scanning rate was 10°/min, and the scanning range was 10 to 80°. The photoluminescence (PL) of ZnAl HTlcs and Tb^{3+}-doped ZnAl HTlcs was analyzed using an F-7000 fluorospectrophotometer. The excitation slit was 2.5 nm and the emission slit 2.5 nm. A 360-nm filter was used.

Results and discussion. *Phase identification analysis.* Figure 1a–d show the XRD patterns of ZnAl HTlcs with different Zn/Al ratios. The results indicate that the synthesized samples were pure, as evaluated by the hexagonal phase of ZnAl HTlcs with the standard diffraction data of JCPDS No. 38-0486 [19, 20]. Figure 1e shows the XRD pattern of a 5% Tb-doped ZnAl hydrotalcite sample. The pattern indicates that a small quantity of Tb^{3+} did not change the hydrotalcite-like phase. The sample was still a pure hydrotalcite-like phase.

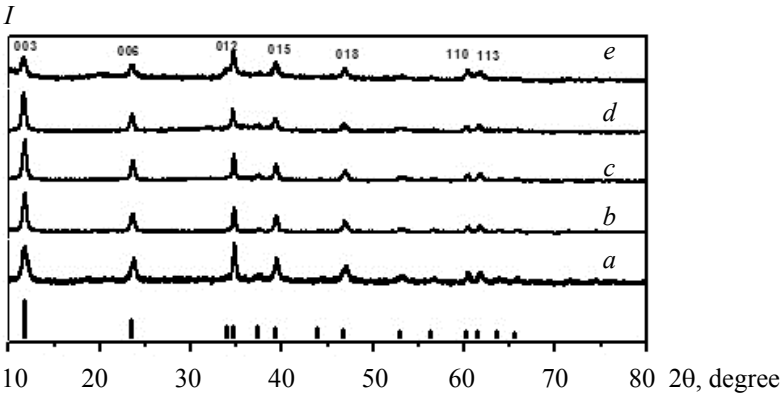

Fig. 1. X-ray diffraction patterns of the samples: (a) $Zn_{1.3}Al$ hydrotalcite-like compound (HTlc); (b) Zn_2Al HTlc; (c) Zn_3Al HTlc; (d) Zn_4Al HTlc; (e) $Zn_{1.3}Al_{0.95}Tb_{0.05}$ HTlc.

Infrared spectra of $Zn_{1.3}Al_{0.95}Tb_{0.05}$ HTlcs. The infrared spectra of the $Zn_{1.3}Al_{0.95}Tb_{0.05}$ HTlcs exhibited the typical characteristic peaks of the hydrotalcite-like sample (Fig. 2). The absorption peaks at 428, 615, and 805 cm^{-1} were attributed to the vibration peaks of metal–oxygen and metal–oxygen–metal (Zn–O, Al–O, and Zn–O–Al) bonds in the Zn–Al LDH compound. The bending vibration peak of the OH group of the crystal water was evident near 1661 cm^{-1} [21]. The broad peak near 3429 cm^{-1} corresponds to the νOH of the hydrotalcite-like sample. The strong absorption peak at 1113 cm^{-1} was attributed to the stretching vibration of SO_4^{2-}. Thus, SO_4^{2-} ions were intercalated in the $Zn_{1.3}Al$ HTlcs and $Zn_{1.3}Al_{0.95}Tb_{0.05}$ HTlcs.

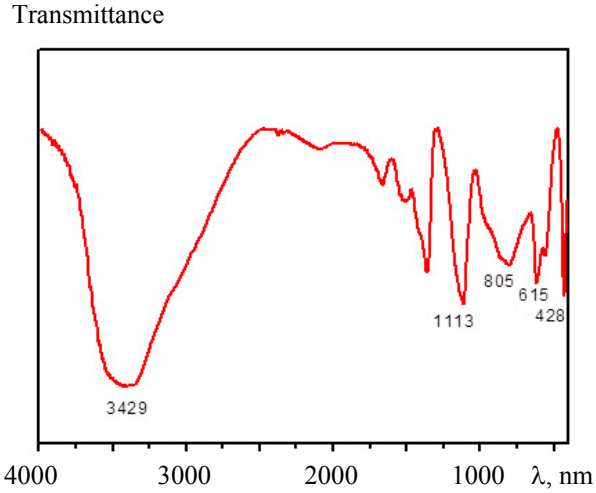

Fig. 2. Fourier-transform infrared spectra of $Zn_{1.3}Al_{0.95}Tb_{0.05}$ hydrotalcite.

Luminescence properties of ZnAl HTlcs. Figure 3 shows the PL spectra of a representative ZnAl HTlc. The maximum emission peak was 399 nm at the maximum excitation peak of 248 nm. Sun et al. also reported ZnAl HTlcs with blue fluorescence, with a maximum emission located at 443 nm at an excitation wavelength of 375 nm [22].

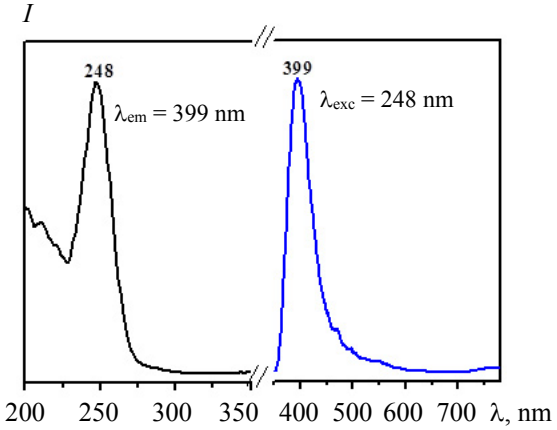

Fig. 3. Excitation and emission spectra of ZnAl hydrotalcite.

Luminescence properties of Zn–Al–Tb HTlcs. Upon excitation into the $4f^8$–$4f^75d^1$ transition at 231 nm, the PL spectra of $Zn_{1.3}Al_{0.95}Tb_{0.05}$ HTlcs exhibited a series of bands because of the $^5D_4 \rightarrow {}^7F_J$ (J = 3–6) of Tb^{3+} ions (Fig. 4) [4–7]. The strongest emission peak was at 547 nm, corresponding to the $^5D_4 \rightarrow {}^7F_5$ transition of Tb^{3+}. Moreover, the weak bands at 350–450 nm originated from the emission of the ZnAl–HTlc matrix. The excitation spectra of Zn–Al–Tb HTlcs were monitored by the 547-nm emission of Tb^{3+} ($^5D_4 \rightarrow {}^7F_5$). The maximum excitation peak was at 231 nm, attributable to the absorption of the charge transfer band between $O^{2-} \rightarrow Tb^{3+}$ (because of the $4f$–$5d$ transition allowed by Tb^{3+}). The excitation peaks at 274 nm were attributed to the spin-forbidden transition of Tb^{3+}, and the remaining weak excitation peaks at 300–400 nm were from $4f^8$ in the shell transition, which is usually very weak [23, 24].

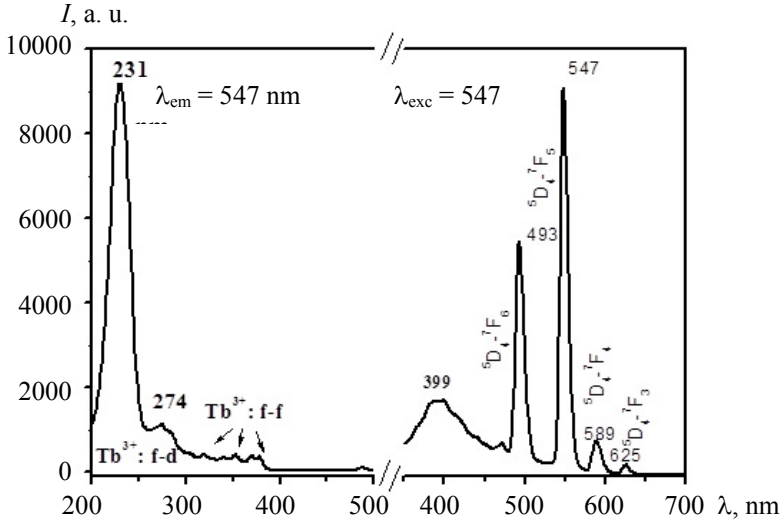

Fig. 4. Excitation and emission spectra of $Zn_{1.3}Al_{0.95}Tb_{0.05}$ HTlcs.

Optimal Zn^{3+}/Al^{3+} ratios and the optimal extent of Tb^{3+} doping. To study the influence of the Zn/Al ratio and the quantity of Tb^{3+} on the luminescence properties, the fluorescence spectra of different ratios and extents of doping were measured at an excitation wavelength of 231 nm (Fig. 5). The fluorescence spectra indicate that the $(Zn^{2+}+Tb^{3+})$/Al ratio of 1.3:1 exhibited the strongest intensity. By increasing the quantity of Tb^{3+} dopant, it was determined that 5% Tb^{3+}-doped ZnAl hydrotalcite exhibited a good intensity. When the quantity of Tb^{3+} was increased to 20%, the intensity of the Tb^{3+} decreased. Therefore, the suitable mole ratio of Zn/Al was 1.3:1, and the suitable quantity of Tb^{3+} dopant was 5%.

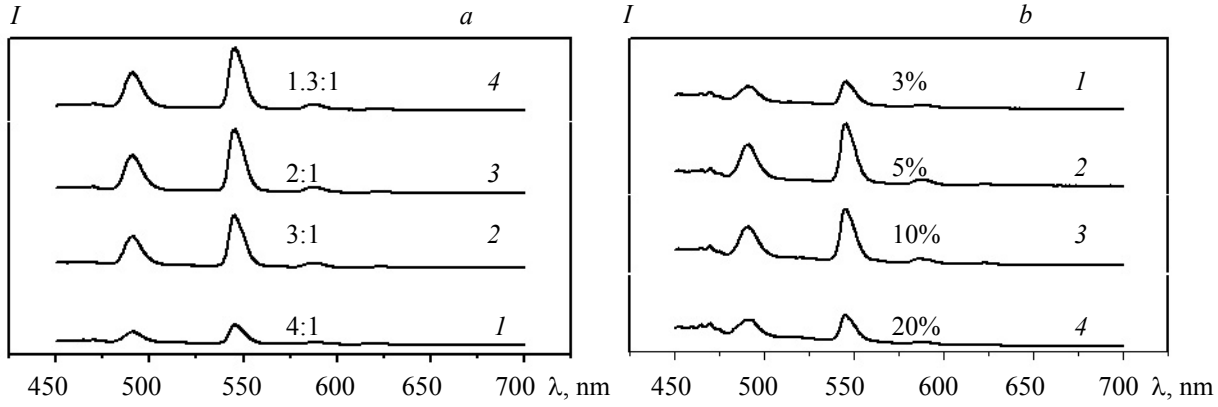

Fig. 5. Photoluminescence emission spectra (λ_{ex} = 231 nm) of samples with (a) various $Zn^{3+}/(Al^{3+})$ ratios and (b) various quantities of Tb^{3+}: a – $Zn_{1.3}Al_{0.95}Tb_{0.05}$ HTlcs (1), $Zn_2Al_{0.95}Tb_{0.05}$ HTlc (2), $Zn_3Al_{0.95}Tb_{0.05}$ HTlc (3), and $Zn_4Al_{0.95}Tb_{0.05}$ HTlc (4); b – $Zn_{1.3}Al_{0.97}Tb_{0.03}$ HTlc (1), $Zn_{1.3}Al_{0.95}Tb_{0.05}$ HTlc (2), $Zn_{1.3}Al_{0.9}Tb_{0.1}$ HTlc (3), and $Zn_{1.3}Al_{0.8}Tb_{0.2}$ HTlc (4).

Decay curves. Figure 6 shows the decay curve of $Zn_{1.3}Al_{0.95}Tb_{0.05}$ HTlc phosphor when the excitation and emission wavelengths were 231 and 547 nm, respectively. The lifetime decay curves perfectly fit the bi-exponential functional equation:

$$y = y_0 + A_1\exp(-x/t_1) + A_2\exp(-x/t_2). \quad (1)$$

The average lifetime was calculated from

$$t_{avr} = \left(A_1t_1 + A_2t_2\right)/\left(A_1 + A_2\right). \quad (2)$$

The fluorescence lifetime of $Zn_{1.3}Al_{0.95}Tb_{0.05}$ HTlc phosphor was 0.8442 ms.

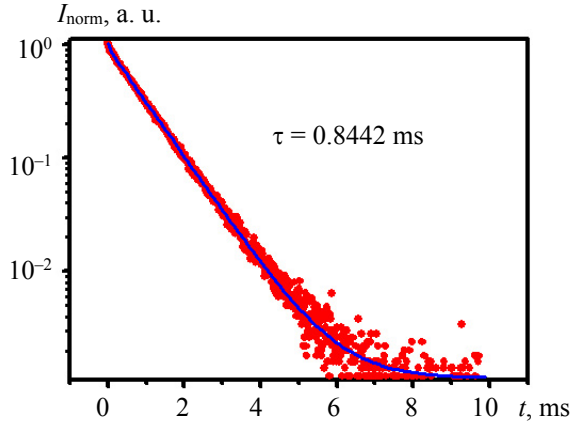

Fig. 6. Room-temperature photoluminescence lifetime decay curve of $Zn_{1.3}Al_{0.95}Tb_{0.05}$ HTlcs phosphor excited at 231 nm. The fit is shown in blue.

Excitation-wavelength-dependent photoluminescence. The luminescence of $Zn_{1.3}Al_{0.95}Tb_{0.05}$ HTlc results from a combination of the emission of the ZnAl–HTlc matrix at 350–450 nm and the $^5D_4 \rightarrow {}^7F_J$ (J = 3–6) green emission of Tb^{3+}. Figure 7 shows the emission spectra of $Zn_{1.3}Al_{0.95}Tb_{0.05}$ HTlcs at various excitation wavelengths. At the maximum excitation wavelength of 231 nm, the sample exhibited strong green fluorescence emission. With increasing excitation wavelength, the blue luminescence intensity of the ZnAl–HTlc matrix increased, whereas the green emission intensity of Tb^{3+} decreased. Under near-UV excitation at 254 nm, the luminescence of the sample exhibited the strong blue fluorescence of the matrix and the weak green fluorescence of the doped terbium ions.

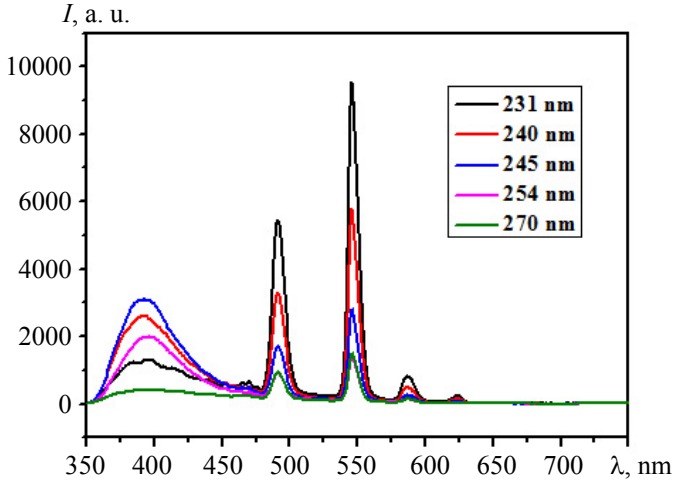

Fig. 7. Excitation-wavelength-dependent photoluminescence of $Zn_{1.3}Al_{0.95}Tb_{0.05}$ HTlcs.

International Commission on Illumination chromaticity coordinates analysis. To observe the color of the phosphor directly, the International Commission on Illumination (CIE) color coordinates were converted in accordance with the spectra. Figure 8 shows the chromaticity diagram. The CIE color coordinates of the ZnAl HTlc phosphor were 0.1721, 0.1009, labeled as "a" in Fig. 8a. ZnAl HTlc exhibited blue emission at an excitation wavelength of 248 nm. The CIE color coordinates of the ZnAlTb HTlcs were calculated to be 0.2323, 0.4508, located in the green region (Fig. 8b). Therefore, ZnAlTb HTlc is a green fluorescent material under UV excitation.

By gradually adjusting the excitation wavelength at 231, 240, 245, and 254 nm, respectively, the corresponding CIE color coordinates gradually changed to 0.2323, 0.4508; 0.2176, 0.3631; 0.1999, 0.2637, and 0.1924, 0.2252; and their luminescence changed from green to sky blue. Thus, they are potential multicolor fluorescent materials. The sample still emitted some green light with color coordinates of 0.2115, 0.3488 at an excitation wavelength of 270 nm, although this is the spin-forbidden transition of Tb^{3+} (Fig. 8d).

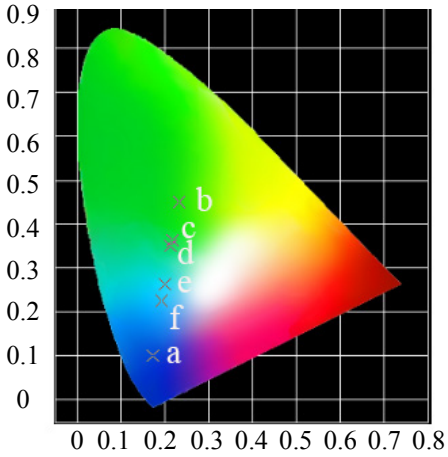

Fig. 8. Chromaticity coordinates of ZnAl hydrotalcite (a) and $Zn_{1.3}Al_{0.95}Tb_{0.05}$ hydrotalcite at various excitation wavelengths: (b) 231 nm; (c) 240 nm; (d) 270 nm; (e) 245 nm; (f) 254 nm.

Conclusions. $Zn_{1.3}Al_{0.95}Tb_{0.05}$ HTlc was synthesized by low-temperature co-precipitation. The $Zn_{1.3}Al_{0.95}Tb_{0.05}$ HTlc exhibited the characteristic emission of Tb^{3+} ions $^5D_4 \rightarrow {}^7F_J$ (J = 3–6) under 231-nm UV excitation. The CIE coordinates of the sample were 0.2323, 0.4508, and the fluorescence lifetime τ was 0.8442 ms. At different excitation wavelengths, the luminescence of $Zn_{1.3}Al_{0.95}Tb_{0.05}$ HTlc gradually changed from green to sky blue; thus, they are potential multicolor fluorescent materials.

Acknowledgments. This work was financially supported by the National Natural Science Foundation of China-Henan (Grant No. U2004193), Henan Provincial Science and Technology Development Funds (No. 222102320057), and Doctor Foundation of Pingdingshan University (PXYBSQD-2015004). We thank the Analytical Center of Pingdingshan University and Changchun Institute of Applied Chemistry for characterizing the samples. We thank Michael Scott Long, PhD, from Liwen Bianji (Edanz) (www.liwenbianji.cn) for editing the English text of a draft of this manuscript.

REFERENCES

1. G. Gouget, M. Pellerin, R. Orabi, *J. Am. Chem. Soc*., **143**, 3300–3305 (2021).
2. R. Galvão, L. F. dos Santos, *J. Phys. Chem. C*, **125**, 14807–14817 (2021).
3. M. Wang, Y. Zhang, *Chem. Mater*., **31**, 5160–5171 (2019).
4. X. Y. Sun, X. X. Fan, J. J. He, *Chin. J. Lumin*., **3**, 36–41 (2020).
5. S. Seiya, T. Izaki, N. Tanaka, Y. Nanai, T. Morimoto, H. Kishimura, *Mater. Res. Bull*., **143**, 111441 (2021).
6. Y. Zhao, S. Wang, Y. J. Han, *J. Lumin*., **223**, 117253 (2020).
7. W. Mi, J. Zheng, Q. Peng, L. Cao, S. Chu, H. Ma, *J. Rare Earths*, **39**, 19–25 (2021).
8. S. Vijay, R. Abhijeet, S. J. Kadam, *Optik*, **243**, 167396 (2021).
9. Q. Wang, D. O. Hare, *Chem. Rev*., **112**, 4124–4155 (2012).
10. W. S. Linghu, H. Yang, Y. X. Sun, *Ind. Eng. Chem. Res*., **247**, 3813–3819 (2008).
11. L. Wan, Z. H. Zhao, X. X. Chen, *ACS Sustain. Chem. Eng*., **8**, 11079–11087 (2020).
12. F. L. Sousa, M. Pillinger, R. Ferreira, *Eur. J. Inorg. Chem*., **4**, 726–734 (2006).
13. Y. Chen, S. Zhou, *J. Solid State Chem*., **183**, 2222–2226 (2010).
14. H. Chen, W. G. Zhang, *J. Am. Ceram. Soc.*, **93**, 2305–2310 (2010).
15. J. P. Liu, X. T. Huang, Y. Y. Li, *J. Phys. Chem. B*, **110**, 21865–21872 (2006).
16. J. C. Yan, M. Zhou, X. L. Pang, *Langmuir*, **35**, 6312–6320 (2019).
17. J. S. Yarger, E. M. P. Steinmiller, K. S. Choi, *Inorg. Chem*., **47**, 5859–5865 (2008).
18. W. Li, W. Q. Xu, M. G. Siebecker, *Environ. Sci. Technol*., **46**, 11670–11677 (2012).
19. X. Yuan, W. Li, *Appl. Clay Sci*., **138**, 107–113 (2017).
20. H. Zhang, L. Nengzi, Z. Wang, X. Zhang, B. Li, X. Cheng, *J. Hazard Mater.*, **383**, 121236 (2020).
21. A. Gandamalla, S. Manchala, A. Verma, et al., *Chemosphere*, **283**, 131182 (2021).
22. S. Sun, W. G. Hou, *Acta Chim. Sin.*, **66**, 155–157 (2008).
23. G. E. Malashkevich, G. I. Semkova, O. L. Amelyanovich, et al., *Opt. Appl.*, **38**, No. 1, 57–63 (2008).
24. J. Yang, C. Zhang, C. Li, et al., *Inorg. Chem.*, **39**, No. 16, 7262–7270 (2010).